Cell Motility and the Cytoskeleton 43:310–321 (1999)

Phosphorylation by CDK1 Regulates XMAP215 Function In Vitro

Robert J. Vasquez,[1] David L. Gard,[2] and Lynne Cassimeris[1]*

[1]*Department of Biological Sciences, Lehigh University, Bethlehem, Pennsylvania*
[2]*Department of Biology, University of Utah, Salt Lake City*

XMAP215, a microtubule-associated protein isolated from *Xenopus* eggs, promotes microtubule assembly dynamics in an end-specific manner: addition of XMAP215 to purified porcine tubulin increases both elongation and shortening rates at microtubule plus ends, with minimal effects at minus ends. Previous results indicated that XMAP215 is phosphorylated during M phase, suggesting that its activity may be regulated by cell cycle phosphorylation. To test this hypothesis, we used video-enhanced DIC microscopy to examine the effects of XMAP215 phosphorylated by CDK1 on the assembly of purified tubulin. XMAP215 incubated with ATP at 30°C for 10– 20 min in the absence of CDK1 exhibited a 4.1-fold increase in plus end elongation rate compared to purified tubulin. Elongation was promoted to a lesser degree (2.4-fold) by phosphorylated XMAP215. In contrast, XMAP215 phosphorylation did not alter the ~3-fold increase in shortening rate. XMAP215 binding to taxol microtubules was also not changed by phosphorylation. To further investigate mechanisms responsible for the faster microtubule shortening rate observed with XMAP215, we made microtubules with segments assembled prior to XMAP215 addition (proximal segments) and segments assembled in the presence of XMAP215 (distal segments). In 9 of 10 microtubules, the distal segment shortened faster (distal = 60.7μm/min; proximal = 37.5μm/min), suggesting that MTs assembled in the presence of XMAP215 have an altered lattice that results in subsequent faster shortening. Cell Motil. Cytoskeleton 43:310–321, 1999.

Key words: microtubules; microtubule associated proteins; dynamic instability; cell cycle

INTRODUCTION

Microtubule (MT) assembly is characterized by periods of elongation and rapid shortening, with abrupt transitions between these states termed catastrophe (the transition between elongation and rapid shortening) and rescue (the transition between rapid shortening and elongation) [Mitchison and Kirschner, 1984; Walker et al., 1988]. This behavior, referred to as dynamic instability, has been observed both in vitro and in vivo [reviewed in Desai and Mitchison, 1997]. Treatment of cells with low doses of taxol, vinblastine, or nocodazole, sufficient to stabilize MTs and prevent turnover, halt, or slow both mitosis and cell locomotion, indicating that MT dynamic turnover is required for these processes [Jordan et al., 1992; Liao et al., 1995; Tanaka and Kirschner, 1991].

Although dynamic instability has been observed both in vitro and in vivo, MTs assembled from purified tubulin in vitro are much less dynamic than those observed in the cytoplasm of living cells [reviewed in

Abbreviations used: CDK1, cyclin dependent kinase 1 ($p34^{cdc2}$); MTs, microtubules; M-phase, meiotic metaphase.

Contract grant sponsor: NSF; Contract grant sponsor: NIH.

R.J. Vasquez's present address is Department of Biochemistry, Joan and Sanford Weil School of Medicine of Cornell University, New York, NY 10021.

*Correspondence to: Lynne Cassimeris, Dept. of Biological Sciences, 111 Research Dr., Lehigh University, Bethlehem, PA 18015. E-mail: lc07@lehigh.edu

Received 21 January 1999; accepted 28 April 1999

Desai and Mitchison, 1997]. For example, in rapidly proliferating vertebrate cells, interphase plus ends elongate about 5–10 times faster than those assembled at comparable concentrations of purified tubulin in vitro [reviewed in Desai and Mitchison, 1997]. This rapid MT assembly in vivo is accompanied by both frequent catastrophes and rescues. Thus, interphase MTs polymerize faster and turn over more quickly than MTs assembled from purified tubulin [Cassimeris et al., 1988].

Regulation of dynamic instability has been postulated to play a major role in both the disassembly of interphase MTs and the assembly of the spindle at mitosis to generate spindle MTs that are both shorter and more dynamic than interphase MTs [reviewed in Hyman and Karsenti, 1996; Desai and Mitchison, 1997]. Studies in living cells have indicated that the average lifetime of MTs decreases dramatically, from approximately 10–15 min to 15–30 sec, during the transition between interphase and mitosis [Saxton et al., 1984]. Additional studies of MT assembly in cells and cytoplasmic extracts indicate that the transition from interphase to mitotic MT dynamics may involve regulation of multiple parameters of dynamic instability, including the rate of elongation [Hayden et al., 1990; Belmont et al., 1990], and the frequencies of catastrophe [Belmont et al., 1990; Verde et al., 1992] and rescue [Gliksman et al., 1992].

It is thought that the dynamic behavior of MTs observed in vivo is modulated by microtubule-associated proteins, or MAPs [reviewed in Hirokawa, 1994]. Although several families of MAPs have been isolated and characterized from vertebrate brain, including MAPs 1, 2, and tau, these brain MAPs suppress dynamic instability and stabilize MTs in vitro [Pryer et al., 1992; Drechsel et al., 1992; Kowalski and Williams, 1993; Vandecandelaere et al., 1996]. This behavior is consistent with the more stable nature of MTs in neuronal cells [Hirokawa et al., 1996]. However, the mechanisms by which MT assembly and dynamics are regulated in non-neuronal cells are less understood.

Recently, examples of several proteins that modulate MT polymerization and dynamics to produce assembly consistent with that observed in rapidly dividing cells have been described. Examples include proteins that promote rescue [MAP4; Ookata et al., 1995], stimulate catastrophes [XKCM1 and Op18; Walczak et al., 1996; Belmont and Mitchison, 1996], and speed plus end elongation without blocking catastrophes [XMAP215; Vasquez et al., 1994]. Several of these proteins are known to be modified by cell cycle–dependent phosphorylation, suggesting that phosphorylation may play an important role in regulating MT assembly dynamics during the transition between interphase and mitosis [reviewed in Desai and Mitchison, 1997; Cassimeris, 1999].

XMAP215 was originally isolated from *Xenopus* eggs based on its ability to promote centrosome-nucleated MT assembly in vitro [Gard and Kirschner, 1987]. XMAP215 has several novel effects on MT dynamics that distinguish it from conventional brain MAPs. For example, unlike other known MAPs that affect assembly of both MT ends, XMAP215 preferentially promotes assembly of MT plus ends. In addition, XMAP215 stimulates both assembly and turnover of MT plus ends by increasing the rates of MT elongation (by 7–10-fold) and rapid shortening (by 3-fold), without a major suppression of catastrophes [Gard and Kirschner, 1987; Vasquez et al., 1994]. Thus, unlike MAPs that reduce dynamic instability and stabilize MTs, XMAP215 promotes the assembly of long and highly dynamic MTs.

Previous studies have demonstrated that XMAP215 is hyper-phosphorylated during meiosis and mitosis in *Xenopus* oocytes and early embryos [Gard and Kirschner, 1987], suggesting that its MT assembly-promoting activity is regulated during the cell cycle. In this report, we have examined the effects of XMAP215 phosphorylation by CDK1 on the ability of this novel MT-associated protein to promote MT assembly and dynamics. Our results reveal that phosphorylation of XMAP215 by CDK1 in vitro diminishes the promotion of MT assembly, without affecting the binding of XMAP215 to taxol-stabilized MTs. Additional results suggest that the promotion of MT disassembly by XMAP215 is dependent upon assembly in the presence of this MAP, suggesting that MTs assembled with XMAP215 have an altered MT lattice structure.

METHODS

Reagents

CDK1 (Cdc2/cyclin B complex) was purchased from Upstate Biologicals Inc. (Lake Placid, NY) or New England Biolabs (Beverly, MA). The CDK1/cyclin B complex provided by Upstate Biologicals Inc. is isolated from the sea star, *Pisaster ochraceus*, while that from New England Biolabs (Boston, MA) is recombinant human CDK1 and cyclin B expressed and purified from Sf9 cells. Creatine kinase was from Boerhinger Mannheim (Indianapolis, IN). All other reagents were from Sigma Chemical Co. (St. Louis, MO) unless otherwise noted.

Protein Purification

XMAP215 was isolated *Xenopus* eggs as described previously [Gard and Kirschner, 1987], with modifications as described in Vasquez et al. [1994]. The final XMAP215 preparations were ~ 90– 95% pure and were dialyzed into PEM buffer (100 mM Pipes, pH 6.9, 2 mM EGTA) supplemented with 200μM PMSF, 1μg/ml phenanthroline, 5μg/ml pepstatin, 1μg/ml benzamidine, and 1

mM DTT. XMAP215 was stored on ice and for all experiments was used within 2 days of the final dialysis step. Most studies were repeated with at least two independent preparations of XMAP215.

Tubulin was purified from porcine brains as described previously [Vasquez et al., 1994] and stored at -80°C. Axonemes were isolated from *Strongylocentrotus purpuratus* or *Chlamydomonas rheinhardtii* [Walker et al., 1988, Witman, 1986], stored at -20°C in 50% glycerol, and washed free of glycerol before use by pelleting and resuspension in PEM buffer.

Xenopus Egg Extracts (100,000*g*)

Cytostatic factor-arrested (M-phase) extracts were prepared from *Xenopus* eggs [Murray, 1991] in CSF-XB (100 mM KCl, 0.1 mM $CaCl_2$, 10 mM K^+Hepes, pH 7.7, 50 mM sucrose, 5 mM EGTA, pH 7.7) and protease inhibitors (10[00b5]g/ml leupeptin, pepstatin, and chymostatin). Interphase extracts were prepared by adding $CaCl_2$ to 0.2 mM and cycloheximide to 100µg/ml and incubating at 20°C for 80 min [Murray, 1991]. The resulting low-speed extracts were clarified at 100,000*g* for 30 min at 22°C in a Beckman (Fullerton, CA) tabletop ultracentrifuge using a TLA 100.2 rotor. Clarified extracts were frozen in liquid nitrogen and stored at -80°C. Cell cycle stage was confirmed by (1) histone H1 phosphorylation [not shown; Murray, 1991], (2) the higher concentration of small vesicles in M-phase extracts [not shown; Parsons and Salmon, 1997], and (3) the reduced ability of M-phase XMAP230 to co-pellet with MTs [Andersen et al., 1994; Fig. 1].

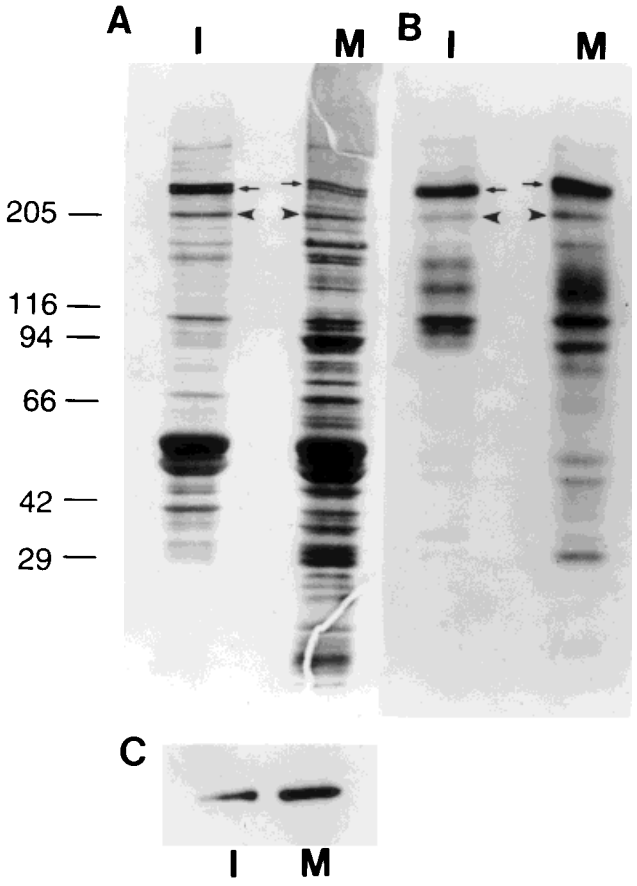

Fig. 1. XMAP215 is phosphorylated in 100,000*g* M-phase *Xenopus* egg extracts. **A:** Silver stained 3–12.5% PAGE gel of proteins co-pelleting with taxol-stabilized MTs in interphase (I) and M-phase (M) *Xenopus* egg extracts. The position of XMAP215 is marked with *arrowheads*, while that of XMAP230 is marked by *small arrows*. XMAP215 co-pellets with MTs in both interphase and M-phase extracts. **B:** Corresponding autoradiogram of the gel shown in A. XMAP215 (*arrowheads*) is weakly phosphorylated in interphase and more highly phosphorylated in M-phase. XMAP230 (*small arrows*) is also phosphorylated in both interphase and M-phase. **C:** Immunoblot of XMAP215 co-pelleting with interphase and M-phase MTs. Blots were probed with an antibody to TOGp, the human homolog of XMAP215 [Charrasse et al., 1998]. The relative increase in M-phase phosphate incorporation for XMAP215 and XMAP230 was measured by scanning densitometry. The relative intensities of bands in the autoradiogram were compared to relative protein levels in either the blot (for XMAP15) or the gel (for XMAP230). At M-phase, XMAP215 has ~ 2-fold higher phosphate, while XMAP230 has ~ 10-fold higher phosphate.

MT Assembly Assays

The assembly of individual MTs from axoneme fragments was visualized with video-enhanced DIC (VE-DIC) microscopy as described previously [Vasquez et al., 1994]. Briefly, axonemes were allowed to adhere to biologically clean coverslips, then assembled into perfusion chambers, using pieces of double stick tape as spacers between slide and coverslip (< 25µl chamber volume), unbound axonemes were removed with 2 chamber volumes PEM/NP-40 (PEM supplemented with 0.5% NP-40), glass surfaces were blocked with 5 mg/ml casein for 2 min, excess casein was removed by perfusion with 2 chamber volumes of PEM/NP-40, and, finally, tubulin/XMAP215 solutions were perfused into the chamber. The tubulin/XMAP215 solutions contained 1 mM GTP, 0.25 mg/ml casein, and 0.5% NP-40 in PEM buffer. Slides were warmed to 35°C on the microscope stage using an air curtain incubator (Nicholson Precision Instruments, Gaithersburg, MD).

Perfusion experiments were used to assemble bipartite MTs containing segments assembled in the absense and presense of XMAP215. *Chlamydomonas* axoneme fragments were used as nucleation sites since these axonemes splay at the plus ends, allowing determination of MT polarity before the addition of XMAP215. Axonemes were first bound to coverslips, the glass surfaces were then blocked with casein as described above, and MTs were assembled from 14–16µM purified tubulin for ~ 5–10 mins in PEM buffer, 1 mM GTP, 0.5% NP-40, and 0.25 mg/ml casein. Solutions containing tubulin (10µM), 1 mM GTP, 0.5% NP-40, 0.25 mg/ml

casein with or without 0.2μM XMAP215 were then perfused into the chamber and MT assembly followed for an additional 10–15 min. One XMAP215 preparation was used for this study. The initial higher tubulin concentration was selected to generate ~ 3–4 MTs per axoneme plus end within a short time frame, while the second perfusion contained a lower concentration of tubulin to increase the likelihood that a catastrophe would occur before the MT elongated out of the field of view. A similar perfusion protocol was used to determine the effects of 1–6 mM $MgCl_2$ on the rate of MT disassembly.

For all experiments, real-time images of MT assembly/disassembly were collected on Super-VHS videotape.

MT Tracking

Rates of MT assembly and disassembly were measured from real-time video sequences using software written by Salmon and colleagues [Gliksman et al., 1992], as described previously [Vasquez et al., 1994]. For statistical analysis of rates of elongation and shortening, analysis of variance (ANOVA) was calculated using Microsoft Excel.

MT Pelleting Assays

To assemble and pellet taxol-stabilized MTs in *Xenopus* extracts, interphase and M-phase extracts were thawed, diluted 1:2 with XMB (10 mM K^+ Hepes, pH 7.7, 50 mM sucrose, 5 mM EGTA, and 10μg/ml of each of the following protease inhibitors: leupeptin, chymostatin, and pepstatin) supplemented with 1 mM ATP, 1 mM $MgCl_2$, 7.5 mM creatine phosphate, and 50μg/ml creatine kinase, and pre-cleared in an airfuge (Beckman) operated at 20 psi for 10 min. The supernatant was removed and incubated with 0.2μCi [^{32}P]-ATP perμl extract and 1μM taxol for 10 min at room temperature. Taxol was then added to a final concentration of 20μM and samples incubated for an additional 20 min at room temperature. MTs and associated proteins were pelleted through a 1-M sucrose cushion (prepared in XMB, supplemented as given above and 10μM taxol) in an airfuge operated at 20 psi for 10 min. Pellets were washed once with XMB and resuspended in gel sample buffer.

MTs were also polymerized at 37°C from 50μM purified tubulin in PEM and 1 mM GTP and stabilized by the addition of taxol in two steps (1μM and 50μM final concentrations). Taxol-stabilized MTs (10μM) were combined with XMAP215, previously phosphorylated as described below, and incubated at 37°C for 10 min. MTs were pelleted (as described above) and pellets washed with PEM before preparing gel samples.

In Vitro Phosphorylation

Purified XMAP215 (0.20μM) in PEM buffer was incubated with 2μM ATP, 2μM DTT, CDK1/cyclin B complex (54 ng/50μl reaction, Upstate Biologicals Inc.; or 333 U/ml, New England Biolabs) for 10 min (for the UBI kinase) or 20 min (for the NEB kinase) at 30°C. Controls were incubated under indentical conditions but without the kinase. For MT assembly assays, samples were held on ice and used in MT assembly assays within 30 min. For MT co-pelleting and autoradiography, the ATP was replaced by 10μCi [^{32}P]-ATP and the phosphorylated protein either used immediately in MT pelleting assays or the reaction was stopped by heating in gel sample buffer.

SDS PAGE, Autoradiography, and Immunoblotting

Proteins were separated on either 7.5% gels (purified XMAP215) or 3–12.5% gradient gels (*Xenopus* extracts). Dried gels were exposed to XAR X-ray film (Kodak, Rochester, NY) with an intensifying screen. The intensity of bands on the X-ray films were measured using a Foto/Analyst Image Analysis System (Fotodyne, Hartland, WI) and Scion Image software (NIH Image and Scion Corp.) run on a Power Macintosh 7100 computer.

For immunoblotting, proteins were transferred to PVDF membranes and probed with rabbit antibodies to TOGp, the human homolog of XMAP215 [Charrasse et al., 1998; antibody generously provided by Dr. C. Larroque). Reactive bands were identified with peroxidase-conjugated secondary antibodies and Enhanced Chemiluminescence (Amersham, Arlington Heights, IL), according to the manufacturer's instructions.

RESULTS

XMAP215 Is Hyper-Phosphorylated in M-phase Xenopus Egg Extracts But Remains Bound to MTs

In the *Xenopus* egg/early embryo, XMAP215 is hyper-phosphorylated at M-phase, with phosphate incorporation increasing ~ 2–3 fold over that in interphase [Gard and Kirschner, 1987]. This cell cycle–dependent hyper-phosphoryation also is detectable *in vitro* in extracts prepared from interphase or M-phase-arrested eggs (see Methods). Extracts were clarified at 100,000*g* and incubated with [^{32}P]-ATP and taxol. The proteins that co-pelleted with MTs are shown in Figure 1A and the corresponding autoradiogram is shown in Figure 1B. Incorporation of radiolabeled phosphate into XMAP215 was observed in both interphase and M-phase extracts. However, in M-phase extracts incorporation of phosphate into XMAP215 was about twofold greater than in similarly treated interphase extracts. This experiment follows only XMAP215 bound to MTs. However, the increase in phosphate incorporation is similar to that measured previously for total XMAP215 in *Xenopus* eggs/early embryos [Gard and Kirschner, 1987].

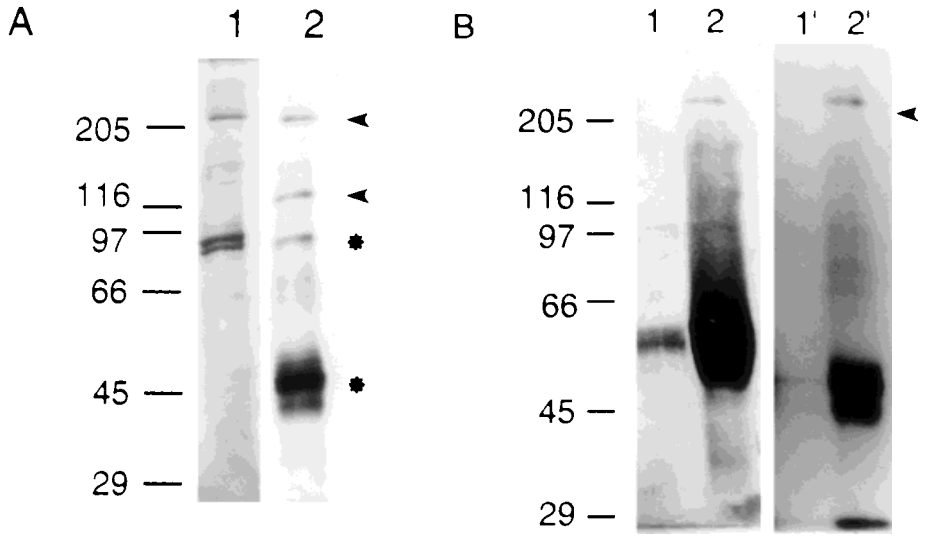

Fig. 2. XMAP215 is phosphorylated by CDK1 in vitro. **A:** Purified XMAP215 was combined with CDK1/cyclin B complex (UBI) and [^{32}P]-ATP for 10 min at 30°C. **Lane 1:** Silver-stained SDS gel of XMAP215 and the kinase complex. **Lane 2:** Corresponding autoradiogram. The position of XMAP215 and a proteolytic fragment of ~ 120 kD are marked with *arrows*. Proteins present in the kinase complex are noted by *astericks;* these proteins are phosphorylated in samples lacking XMAP215. **B:** Phosphorylated XMAP215 co-pellets with MTs. Phosphorylated XMAP215 was combined with taxol-stabilized MTs and pelleted through a sucrose cushion. The resulting supernatants (**lanes 1** and **1'**) and pellets (**lanes 2** and **2'**) are shown for a silver stained gel (lanes 1 and 2) and the corresponding autoradiogram (lanes 1' and 2'). Positions of Mr markers are shown.

Surprisingly, M-phase phosphorylation did not decrease the ability of XMAP215 to co-pellet with MTs. Both SDS PAGE (Fig. 1A) and immunoblotting (Fig. 1C) revealed that equivalent amounts of XMAP215 cosedimented with MTs in both interphase and M-phase extracts. In contrast, cosedimentation of XMAP230, a potent MT stabilizer [Andersen et al., 1994] that is hyperphosphorylated in M-phase, with MTs is greatly reduced in M-phase extracts (Fig. 1A,B), consistent with previous studies [Andersen et al., 1994].

XMAP215 Is Phosphorylated by CDK1 In Vitro

Since XMAP215 is hyper-phosphorylated during M-phase, we next asked whether it was a substrate for CDK1. Purified XMAP215 was incubated in vitro with $^{32}PO_4$-labeled ATP and commercially prepared CDK1/cyclin B (two commercial CDK1/cyclin B preparations were used with identical results). As shown in Figure 2A, radiolabeled phosphate was incorporated into XMAP215 in the presence of CDK1, but not in its absence, indicating that XMAP215 is a substrate for CDK1 in vitro. Incorporation of $^{32}PO_4$ into a breakdown product of XMAP215 (~ 120 kD) was also observed under these conditions. Several additional radiolabeled bands observed in the autoradiogram shown in Figure 2A represent phosphorylated components in the kinase preparations, since they are also detected in the absence of added XMAP215 (not shown).

XMAP215 phosphorylated in vitro by CDK1 co-pelleted with MTs (Fig. 2B), consistent with the results obtained in *Xenopus* egg extracts (Fig. 1). A ~ 47 kDa protein present in the commercial kinase preparation also co-pelleted with MTs (Fig. 2A) and was highly phosphorylated (Fig. 2B). The intensity of this band was significantly lower in additional experiments (data not shown). We have not yet identified this phospho-protein.

Phosphorylation of XMAP215 Reduces Its Assembly-Promoting Activity

To assay the effect of XMAP215 phosphorylation on MT assembly promotion and dynamics, we incubated XMAP215 with CDK1/cyclin B and ATP at 30°C for 10–20 min, and assayed MT assembly dynamics by video-enhanced DIC microscopy. We compared the activity of the in vitro phosphorylated XMAP215 to parallel samples of XMAP215 incubated with ATP at 30°C in the absence of the kinase (referred to as unphosphorylated XMAP215), and to unmanipulated XMAP215 from the same preparation (control XMAP215). Phosphorylated or unphosphorylated XMAP215 (to a final concentration 0.15μM) was added to 10μM tubulin, and MT assembly from axoneme fragments was examined.

Under the conditions used for these experiments, 0.2μM unmanipulated (control) XMAP215 promoted a ~5-fold increase in the rate of plus-end elongation (compared to tubulin alone) with little or no effect on the

TABLE I. CDK Phosphorylation Modifies XMAP215 Activity*

	Tb	Tb + XMAP215	Tb + XMAP215-PO4
V_e (μm/min) ± s.d.	1.14 ± 0.52	4.72 ± 1.79	2.71 ± 1.38
n	41	32	45
V_{rs} (μm/min) ± s.d.	19.4 ± 12.0	56.4 ± 17.8	63.7 ± 20.3
n	31	26	31
K_{cat} (s^{-1})	0.0122 ± 0.002	0.0154 ± 0.0030	0.0126 ± 0.0023
n	33	26	31
Avg L (μm)[a]	1.56	5.11	3.58

*Changes in microtubule plus end assembly dynamics after addition of XMAP215 with or without CDK1 phosphorylation. All samples contained 10 μM total tubulin ±0.15 μM XMAP215. V_e, elongation velocity; V_{rs}, shortening velocity; K_{cat}, catastrophe frequency; s.d., standard deviation; n, number of microtubules (V_e or V_{rs}) or catastrophes. The data were pooled from two XMAP215 and tubulin preparations.

[a]Average length of microtubules before catastrophe, calculated based on $V_e \times 1$/catastrophe frequency.

minus end, consistent with our previously published results [Vasquez et al., 1994] (data not shown). Incubation of XMAP215 with ATP in the absence of kinase (unphosphorylated XMAP215) had little effect on its ability to promote MT elongation: 0.15μM unphosphorylated XMAP215 stimulated assembly 4.1-fold compared to tubulin alone (Table I). Since ATP was included in the reaction mixture, these results suggest that the biochemically-purified XMAP215 preparation does not contain any residual protein kinases capable of altering XMAP215 activity. In contrast, XMAP215 incubated with ATP and CDK1/cyclin B (0.15μM phosphorylated XMAP215) only promoted plus-end elongation ~2.4-fold (relative to tubulin alone), yielding assembly rates about half those obtained with comparable amounts of unphosphorylated XMAP215. Statistical analysis revealed that the differences in MT elongation rates measured in the presence of unphosphorylated XMAP215, phosphorylated XMAP215, or tubulin alone, were statisically significant ($P < 0.01$).

Previously, we reported that the plus ends of MTs assembled with XMAP215 shorten approximately 3 times faster than MTs assembled from purified tubulin [Vasquez et al., 1994]. In the current study, the average plus end shortening rate for MTs assembled from tubulin alone was 19.4μm/min (Table I). MTs assembled in the presence of unphosphorylated XMAP215 depolymerized at a mean rate of 56.3μm/min (Table I), consistent with our previous results [Vasquez et al., 1994]. This increased shortening velocity is statistically significant ($P < 0.01$). MTs assembled in the presence of phosphorylated XMAP215 disassembled at a mean rate of 63.7 μm/min (Table I), indicating that phosphorylation of XMAP215 had no effect on the ability of XMAP215 to enhance the shortening rate at the plus ends of MTs.

Phosphorylation of XMAP215 also did not change catastrophe frequency at the plus ends of MTs, when calculated as events per unit time. The catastrophe frequency for the plus ends of MTs assembled from tubulin alone was approximately one every 82 sec, and catastrophes were observed with similar frequency in samples containing unphosphorylated or phosphorylated XMAP215 (Table I). We also calculated the average length that MTs would grow to prior to catastrophe, since MTs with different growth rates will incorporate different numbers of subunits even with similar catastrophe frequencies. Thus, MTs assembled from 10μM tubulin grew to a mean length of 1.56μm before catastrophe. In the presence of 0.15 μM of unphosphorylated XMAP215, MTs assembled to a mean length of 5.11μm, while addition of a comparable amount of phosphorylated XMAP215 resulted in MTs with a mean length of 3.58μm. Consistent with our previous results [Vasquez et al., 1994], plus ends assembled with XMAP215 shorten completely back to the nucleation site without rescue. This same result was observed with both phosphorylated and unphosphorylated XMAP215 (data not shown).

XMAP215 had lesser effects on minus end assembly. Consistent with previous studies [Gard and Kirschner, 1987; Vasquez et al., 1994], both phosphorylated and unphosphorylated XMAP215 increased minus end elongation rate ~1.8-fold (data not shown). Minus end MTs assembled with either phosphorylated or unphosphorylated XMAP215 shortened at approximately the same rate as those assembled from purified tubulin (data not shown).

XMAP215 Enhancement of Plus End Shortening Rate Requires MT Assembly in the Presence of XMAP215

Since the ability to increase the rate of plus end shortening velocity is unique to XMAP215, we investigated possible mechanisms responsible for this enhanced rate of shortening. Two mechanisms could generate the faster plus end shortening observed with XMAP215: first, interaction of XMAP215 with tubulin in the walls of MTs could alter the MT lattice in a manner that enhances the shortening velocity (for example, by decreasing lateral interactions between tubulin subunits); alternatively, *as-*

sembly of MTs in the presence of XMAP215 could alter the MT lattice in a manner that favors rapid disassembly.

To distinguish between these possibilities, we assembled bipartite MTs in which the segments proximal to the axoneme were assembled in the absence of XMAP215 (but XMAP215 could bind after assembly) and segments distal to the axoneme were assembled in the presence of XMAP215. We then examined the rates of disassembly of the distal portion of such bipartite MTs, assembled in the presence of XMAP215, compared to the proximal portion to which XMAP215 should have bound after MT assembly. Note that all experiments used unmanipulated (not phosphorylated) XMAP215.

An example of this experiment is shown in Figure 3. Initially, the MT assembles at a relatively slow velocity and this increases when a solution containing XMAP215 and tubulin is perfused into the chamber. Once this MT undergoes a catastrophe, it shortens completely back to the nucleation site. As evident in the length vs. time plot, the distal segment of the MT shortens faster than the proximal segment (Fig. 3A and B), suggesting that assembly in the presence of XMAP215 is required for subsequent faster shortening.

A total of 10 MTs were successfully followed throughout perfusion experiments. For 9 of the 10 MTs, the proximal MT segment shortened at a slower velocity than the distal MT segment. The remaining MT shortened at an intermediate velocity over its entire length. The average shortening velocities of MT segments proximal and distal to the axoneme are shown in Figure 3C. The distal segment, assembled in the presense of XMAP215, showed the expected fast shortening rate of 60.7μm/min (s.d. = ± 17.9). In contrast, the proximal segment, which should be bound by XMAP215 after assembly, shortened at a significantly ($P < 0.01$) slower velocity (37.5μm/min, s.d. = ± 12.1). The proximal MT segments shortened slightly faster than MTs assembled from purified tubulin (30.2μm/min, s.d. = ± 19.9 for this tubulin preparation), but these rates were not significantly different.

High concentrations of magnesium (e.g., 6 mM) have also been reported to increase the rate of MT shortening [O'Brien et al., 1990]. This is thought to be due to interaction of magnesium with the preformed MT lattice [O'Brien et al., 1990], suggesting that bipartite MTs assembled at low (1 mM) and high (6 mM) magnesium would show fast shortening for both distal and proximal MT segments. This was observed: proximal and distal segments shortened at average velocities of 85–90μm/min (n = 6 MTs, not shown). These results suggest that the differences in shortening velocity observed in the XMAP215 experiments were not a consequence of perfusion or the assembly of bipartite MTs.

DISCUSSION

CDK1 Phosphorylation of XMAP215 Decreases Elongation Promoting Activity Without Decreasing MT Binding

Phosphorylation of XMAP215, whether by endogenous kinases in cytoplasmic extracts or by purified CDK1, had no apparent affect on the ability of XMAP215 to bind to taxol-stabilized MTs in vitro. This contrasts with the reported effects of phosphorylation of other MAPs, including tau, MAP2, E-MAP-115, and XMAP230, where phosphorylation or hyper-phosphorylation resulted in decreased binding to MTs and, when measured, decreased MT-stabilization [Jameson and Caplow, 1981; Lindwall and Cole, 1984; Hoshi et al., 1992; Shiina et al., 1992; Masson and Kreis, 1995; Andersen et al., 1994]. However, decreased affinity for MTs is not a universal result of MAP phosphorylation. For example, both tau and MAP2 are phosphorylated at multiple sites, yet phosphorylation-dependent effects on MT affinity are limited to a subset of these sites [Trinczek et al. 1995; Brugg and Matus, 1991]. In addition, phosphorylation of MAP4 eliminates its ability to promote MT rescues, but does not alter MT binding [Ookata et al, 1995].

While not affecting binding to taxol-stabilized MTs, phosphorylation of XMAP215 by CDK1 in vitro significantly reduces, but does not eliminate, the promotion of plus end elongation by XMAP215 (Table I). Interestingly, phosphorylation of XMAP215 by CDK1 reduces promotion of MT elongation to levels similar to that observed with other, well-studied, neuronal MAPs [Drechsel et al., 1992; Pryer et al., 1992; Trinczek et al., 1995; Kowalski and Williams, 1993; Vandecandelaere et al., 1996]. Thus, while phosphorylation by CDK1 does not eliminate the ability of XMAP215 to promote MT assembly, phosphorylated XMAP215 appears to act similarly to more conventional MAPs. Phosphorylation of XMAP215 had little effect on the promotion of minus end assembly. Thus, the phosphorylation-dependent reduction in the ability of XMAP215 to promote plus end growth reduces, or eliminates, the striking plus-end specificity of unphosphorylated XMAP215.

Although the mechanisms by which brain MAPs promote MT elongation remain controverisal [Drechsel et al., 1992], results from several studies suggest that MAPs 1, 2, and tau increase the rate of MT elongation by decreasing the dissociation of tubulin subunits from the MT end [Pryer et al., 1992; Trinczek et al., 1995; Vandecandelaere et al., 1996]. This mechanism is insufficient to account for the dramatic promotion of plus-end elongation observed with unphosphorylated XMAP215 [Gard and Kirschner, 1987; Vasquez et al., 1994]. However, it might explain the reduced promotion of MT

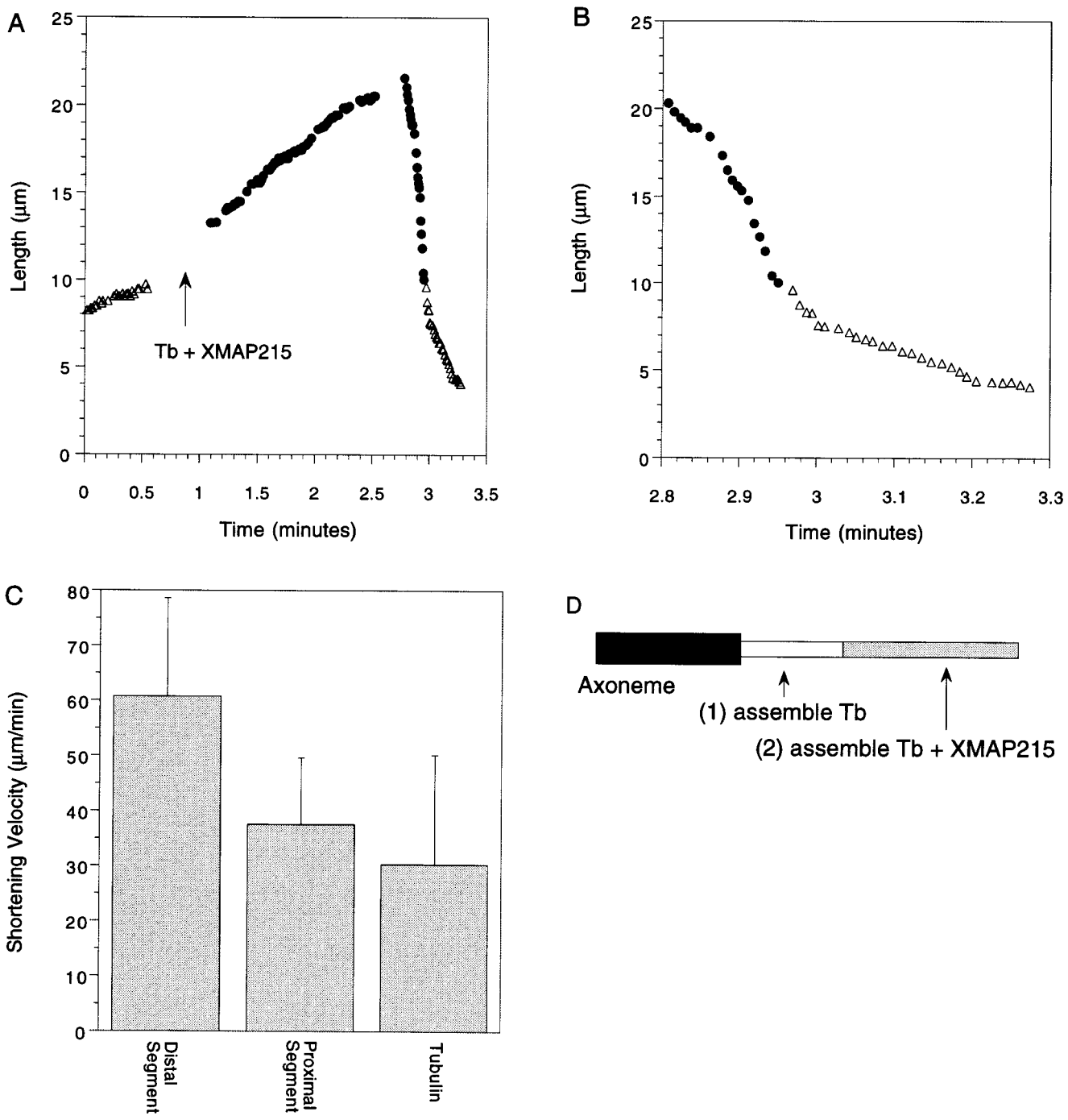

Fig. 3. Fast plus end shortening requires MT assembly in the presense of XMAP215. Bipartite MTs were assembled from purified tubulin (proximal segment) followed by assembly in both tubulin and XMAP215 (distal segment; see text for details). **A:** Elongation and shortening of a single plus end MT. Perfusion of a solution containing tubulin and XMAP215 results in faster elongation. This MT then catastrophes and shortens at an initial fast rate (corresponding to the distal segment) followed by shortening at a slower rate (corresponding to the proximal segment). An enlargement of the shortening portion of the curve is shown in **B**. **C:** Histogram showing mean rates of shortening ± s.d. for distal and proximal MT segments compared to that measured for purified tubulin. n's = 10, 10, 27. **D:** Drawing depicting the experimental protocol. Tubulin was first allowed to assembled into MTs (i.e., the *open triangles* in A). A solution of tubulin plus XMAP215 was then perfused into the chamber to generate distal ends of MTs assembled in the presense of XMAP215 (i.e., the *closed circles* in B). MTs were observed until they switched to the shortening phase.

elongation velocities and lack of end-specificity observed with phosphorylated XMAP215.

Although XMAP215 may share some similarities with the neuronal MAPs, its binding interaction with MTs is likely different from these MAPs since XMAP215 both speeds plus end shortening rate and does not promote rescues [Vasquez et al., 1994]. These activities are also unaffected by phosphorylation.

The observation that phosphorylation by CDK1 does not reduce the ability of XMAP215 to bind MTs suggests that phosphorylated XMAP215 is still able to bind MTs and modulate MT dynamics. This conclusion is further supported by our observation that phosphorylation by CDK1 reduces, but does not eliminate, the effect of XMAP215 on MT assembly. However, we have not measured the extent or stoichiometry of XMAP215 phosphorylation in our in vitro experiments. Thus, we cannot rule out the possibility that the residual growth promotion observed with ''phosphorylated'' XMAP215 was due to a fraction of the XMAP215 that remained unphosphorylated. Despite this caveat, our results demonstrate that phosphorylation of XMAP215 by CDK1 reduces the ability of XMAP215 to promote MT elongation at the plus end, providing further support for the hypothesis that cell cycle–dependent phosphorylation regulates XMAP215 activity in vivo [Gard and Kirschner, 1987].

Enhancement of Rapid Shortening Is Dependent on MT Assembly in the Presence of XMAP215

MT plus-ends assembled in the presence of XMAP215 shorten faster than plus ends assembled from tubulin alone [Vasquez et al., 1994] (Table I) and faster than ends to which XMAP215 is added after assembly (Fig. 3). We have not directly demonstrated that XMAP215 binds to the proximal MT segment in these experiments. However, XMAP215 binds to pre-assembled taxol-stabilized MTs at a ratio of 1 XMAP215:13 tubulin heterodimers [Gard and Kirschner, 1987] demonstrating that XMAP215 can bind to a preformed MT lattice. Preliminary reports have suggested that XMAP215 has a higher affinity for MT ends [Jain et al.. 1997]. In the current study, the concentration of XMAP215 (0.2μM) was well in excess of the MT polymer concentration (estimated at $< 0.01\mu M$), suggesting that XMAP215 is present at sufficient concentration to saturate the MT polymer, even if it has a higher affinity for MT ends. Thus, our results suggest that enhancement of rapid shortening is dependent upon assembly in the presence of XMAP215, and does not result from subsequent binding of XMAP215 to the MT lattice.

The ability of XMAP215 to promote the rapid shortening of MT plus-ends is unique, and has not been observed with any other MAP or protein factor affecting MT dynamics. The mechanism by which XMAP215 enhances shortening velocity remains unknown. However, MT protofilaments have been observed peeling away from the MT lattice during shortening [Mandelkow et al., 1991], consistent with the hypothesis that the lateral interactions between protofilaments are weaker than those along the protofilament. We postulate that the assembly of MT plus ends in the presence of XMAP215 alters the MT lattice in such a way that inter-protofilament bonds are weakened further, resulting in MTs that peel apart faster. Confirmation of this model will require biophysical and structural analysis of the interactions between XMAP215 and tubulin, and between tubulin subunits assembled in the presence of XMAP215.

XMAP215 Is Sufficient to Account for the Rates of MT Elongation and Shortening Observed in High-Speed Xenopus Egg Extracts

The dramatic promotion of MT elongation by XMAP215 may reflect the unique requirements of regulating MT assembly and organization in large cells such as *Xenopus* eggs (with diameters of 1.2 mm). Although the rates of MT assembly in intact *Xenopus* eggs have not been measured (due to microscopic limitations caused by their size and opaque cytoplasm), assembly rates of 25–50μm/min have been estimated based on the time required to assemble the sperm aster and cortical MTs during the first cell cycle after fertilization [Gard, 1992; Stewart-Savage and Grey, 1992]. These estimates are 5–10-fold higher than rates of MT assembly measured in smaller, cultured somatic cells [e.g., Cassimeris et al., 1988; Sammak and Borisy, 1988].

To circumvent the problems of measuring MT dynamics in intact eggs, several studies have examined MT assembly and dynamics in cytoplasmic extracts prepared from *Xenopus* eggs [Belmont et al., 1990; Parsons and Salmon, 1997; Tournebize et al., 1997; Waterman-Storer et al., 1995]. MT elongation rates in interphase extracts ranged from 10μm/min to 23μm/min [Belmont et al., 1990; Parsons and Salmon, 1997; Tournebize et al., 1997; Waterman-Storer et al., 1995] while mitotic extracts supported microtubule elongation at rates of 10–12μm/min [Belmont et al., 1990; Parsons and Salmon, 1997; Tournebize et al., 1997]. The microtubule elongation rate either slowed in mitotic extracts compared to that in interphase extracts [Parsons and Salmon, 1997; Tournebize et al., 1997], or was similar in both cell cycle stages [Belmont et al., 1990]. Although not uniformly observed, the faster rate of MT assembly measured in interphase extracts [Parsons and Salmon, 1997; Tournebize et al., 1997] may reflect unique requirements for rapid MT assembly in the *Xenopus* egg; in vertebrate tissue cells MT growth rate is faster during mitosis compared to that in interphase [Hayden et al., 1990]. MT

TABLE II. XMAP215 Is Sufficient to Generate the Rates of MT Assembly in High-Speed *Xenopus* Egg Extracts*

	Clarified *Xenopus* egg extract[a]	Tb + XMAP215[b]
Interphase		
V_e (μm/min)	17–22 μm/min	18–22 μm/min
V_{rs} (μm/min)	55–58 μm/min	50–60 μm/min
M-Phase		
V_e (μm/min)	10–11 μm/min	10–12 μm/min
V_{rs} (μm/min)	67 μm/min	64 μm/min

*V_e, elongation velocity; V_{rs}, shortening velocity.

[a]Data from 100k × g or 218k × g clarified *Xenopus* egg extracts observed by VE-DIC microscopy, from Waterman-Storer et al. [1995] and Parsons and Salmon [1997].

[b]Extrapolated to 20–25 μM tubulin (as measured in clarified *Xenopus* extracts) [Parsons and Salmon, 1997]. Interphase elongation velocities were calculated based on rate constants determined previously [Vasquez et al., 1994] and M-phase elongation velocities are 57% of these values (based on Table I). Shortening velocities for unphosphorylated XMAP215 combine data presented here and rates measured previously [Vasquez et al., 1994].

shortening velocities differed in extracts prepared by high- or low-speed clarification: rates of 55–67μm/min were measured in high-speed extracts [Parsons and Salmon, 1997; Waterman-Storer et al., 1995], compared to rates of 13–18μm/min measured in low-speed extracts [Belmont et al., 1990; Tournebize et al., 1997]. It is possible that a MT stabilizer has been lost during clarification at the higher g force, resulting in a faster disassembly rate.

The rates of MT shortening observed with purified XMAP215 and tubulin (55– 63μm/min) are similar to the MT shortening rates measured in high speed extracts (55–67μm/min) [Waterman-Storer et al., 1995; Parsons and Salmon, 1997] (Table II). Interestingly, shortening is slightly faster in M-phase extracts and CDK1-phosphorylated XMAP215 also generates slightly faster shortening velocities in vitro (Table II). Thus, XMAP215 is sufficient to account for the fast MT shortening rates observed in high-speed extracts.

The rates of MT elongation we observe in vitro with purified XMAP215 and tubulin, when extrapolated to the tubulin concentration present in *Xenopus* eggs and extracts, are also similar to those observed in Xenopus extracts. For example, MTs in high-speed interphase extracts elongated at 17–22μm/min [Waterman-Storer et al., 1995; Parsons and Salmon, 1997] compared to 18–22μm/min extrapolated from rates measured for purified XMAP215 and tubulin (Table II). Similarly, MTs in M-phase high speed extracts elongated at 10–11μm/min [Parsons and Salmon, 1997] compared to 10–12μm/min extrapolated from the rates measured with purified tubulin and CDK1-phosphorylated XMAP215 (Table II). Our extrapolated elongation rates also match well with rates measured in low speed extracts by Tournebize et al. [1997] (16.5μm/min in interphase and 11μm/min in metaphase). The correspondence between the observed rates of MT elongation obtained with cytoplasmic extracts and purified XMAP215 and tubulin suggests that XMAP215 is the primary factor stimulating fast elongation in extracts.

The postulated role of of XMAP215 in regulating MT elongation and shortening is consistent with the observed effects of immunodepletion of XMAP215 on MT assembly in cytoplasmic extracts. Tournebize et al. [Tournebize et al., 1998] reported that partial depletion (~75% reduction) of XMAP215 reduced MT elongation and shortening rates in interphase extracts. In contrast, interphase extracts nearly completely depleted of XMAP230, another major MAP present in Xenopus eggs, showed no change in MT elongation rate [Cha et al., 1998]. While other factors, such as Op18/stathmin [Belmont and Mitchison, 1996], XKCM1 [Walczak et al., 1996], and XMAP230 [Andersen et al., 1994] undoubtedly play roles in regulating MT dynamics and organization, these observations suggest that XMAP215 is predominately responsible for the fast rate of MT elongation, and perhaps the rate of shortening, in *Xenopus* eggs.

In summary, our results indicate that phosphorylation of XMAP215 by CDK1 modulates XMAP215 function, suggesting that cell cycle–dependent phosphorylation of XMAP215 by CDK1 might play an important role in the regulation of MT dynamics during the transition from interphase to M-phase, perhaps by contributing to changes in MT length. Recently, sequencing of cDNAs encoding XMAP215 cloned from *Xenopus* oocyte mRNA revealed that XMAP215 protein contains two strongly predicted target sequences for CDK1-dependent phosphorylation (Becker and Gard, unpublished data). Future studies will be required to determine whether one or both phoshorylation sites are necessary for regulation of XMAP215 by CDK1 during the cell cycle.

ACKNOWLEDGMENTS

Thanks to Dr. Christian Larroque for providing antibodies to TOGp. L.C. is grateful to Dr. Sandra Holloway for help preparing *Xenopus* egg extracts, Arsad Desai for advice on assembling taxol MTs in *Xenopus* extracts, and Mike Kuchka for providing *Chlamydomonas*. This work was supported by grants from NSF (D.L.G.) and NIH (L.C.).

REFERENCES

Andersen SL, Buendia B, Dominguez JE, Sawyer A, Karsenti E. 1994. Effect on microtubule dynamics of XMAP230, a microtubule-associated protein present in *Xenopus laevis* eggs and dividing cells. J. Cell Biol. 127:1289–1299.

Belmont L, Mitchison T. 1996. Identification of a protein that interacts with tubulin dimers and increases the catastrophe rates of microtubules. Cell 84:623– 631.

Belmont LD, Hyman AA, Sawin KE, Mitchison TJ. 1990. Real time visualization of cell cycle dependent changes in microtubule dynamics in cytoplasmic extracts. Cell 62:579–589.

Brugg B, Matus A. 1991. Phosphorylation determines the binding of microtubule-associated protein 2 (MAP2) to microtubules in living cells. J Cell Biol 114:735–743.

Cassimeris L. 1999. Accessory protein regulation of microtubule assembly dynamics throughout the cell cycle. Curr Opin Cell Biol 11:134–141.

Cassimeris L, Pryer NK, Salmon ED. 1988. Real-time observations of microtubule dynamic instability in living cells. J Cell Biol 107: 2223–2231.

Cha B-J, Cassimeris L, Gard DL. 1998. XMAP230 is required for normal spindle assembly and stabilizing spindle microtubules. Mol Biol Cell 9:157a.

Charrasse S, Schroeder M, Gauthier-Rouviere C, Ango F, Cassimeris L, Gard DL, Larroque C. 1998. The TOGp protein is a new human microtubule-associated protein homologous to the Xenopus XMAP215. J Cell Sci 111:1371–1383.

Desai A, Mitchison T. 1997. Microtubule polymerization dynamics. Ann Rev Cell Biol 13:83–117.

Drechsel DN, Hyman AA, Cobb MH, Kirschner MW. 1992. Modulation of the dynamic instability of tubulin assembly by the microtubule-associated protein tau. Mol Biol Cell 3:1141–1154.

Gard DL. 1992. Microtubule organization during maturation of Xenopus oocytes: Assembly and rotation of the meiotic spindles. Dev Biol 151: 516–530.

Gard DL, Kirschner MW. 1987. A microtubule-associated protein from *Xenopus* eggs that specifically promotes assembly at the plus-end. J Cell Biol 105: 2203– 2215.

Gliksman N, Parsons SF, Salmon ED. 1992. Okadaic acid induces interphase to mitotic-like microtubule dynamic instability by inactivating rescue. J Cell Biol 119:1271–1276.

Hayden J, Bowser SS, Rieder CL. 1990. Kinetochores capture astral microtubules during chromosome attachment to the mitotic spindle: Direct visualization in live newt lung cells. J Cell Biol 111:1039–1045.

Hirokawa N. 1994. Microtubule organization and dynamics dependent on microtubule-associated proteins. Curr Opin Cell Biol 6:74–81.

Hirokawa N, Funakoshi T, Sato-Harada R, Kanai Y. 1996. Selective stabilization of tau in axons and microtubule-associated protein 2C in cell bodies and dendrites contributes to polarized localization of cytoskeletal proteins in mature neurons. J Cell Biol 132:667–679.

Hoshi M, Ohta K, Gotoh Y, Mori A, Murofushi H, Sakai H, Nishida E. 1992. Mitogen-activated-protein-kinase-catalyzed phosphorylation of microtubule-associated proteins, microtubule-associated protein 2 and microtubule-associated protein 4, induces an alteration in their function. Eur J Biochem 203: 43–52.

Hyman AA, Karsenti E. 1996. Morphogenetic properties of microtubules and mitotic spindle assembly. Cell 84:401–410.

Jain SK, Mitchison TJ, Podtelezhnikov A, Mann M, Hyman AA. 1997. Identification of microtubule-end binding proteins. Mol Biol Cell 8:48a.

Jameson L, Caplow M. 1981. Modification of microtubule steady-state dynamics by phosphorylation of the microtubule-associated proteins. Proc Natl Acad Sci USA 78:3413–3417.

Jordan MA, Thrower D, Wilson L. 1992. Effects of vinblastine, podophyllotoxin and nocodazole on mitotic spindles: implications for the role of microtubule dynamics in mitosis. J Cell Sci 102:401–416.

Kowalski RJ, Williams RC. 1993. Microtubule-associated protein 2 alters the dynamic properties of microtubule assembly and disassembly. J Biol Chem 268:9847–9855.

Liao G, Nagasaki T, Gundersen GG. 1995. Low concentrations of nocodazole interfer with fibroblast locomotion without signficantly affecting microtubule level: implications for the role of dynamic microtubules in cell locomotion. J Cell Sci 108:3473–3483.

Lindwall G, Cole DR. 1984. Phosphorylation affects the ability of tau protein to promote microtubule assembly. J Biol Chem 259: 5301–5305.

Mandelkow EM, Mandelkow E, Milligan RA. 1991. Microtubule dynamics and microtubule caps: A time-resolved cryo-electron microscopy study. J Cell Biol 114: 977–991.

Masson D, Kries TE. 1995. Binding of E-MAP-115 to microtubules is regulated by cell cycle-dependent phosphorylation. J Cell Biol 131:1015–1024.

Mitchison T, Kirschner M. 1984. Dynamic instability of microtubule growth. Nature 312:237–242.

Murray AW. 1991. Cell cycle extracts. Methods Cell Biol 36:581–605.

O'Brien ET, Salmon ED, Walker RA, Erickson HP. 1990. Effects of magnesium on the dynamic instability of individual microtubules. Biochemistry 29:6648–6656.

Ookata K, Hisanaga S, Bulinski JC, Murofushi H, Aizawa H, Itoh TJ, Hotani H, Okumura E, Tachibana K, Kishimoto T. 1995. Cyclin B interaction with microtubule-associated protein 4 (MAP4) targets $p34^{cdc2}$ kinase to microtubules and is a potential regulator of M-phase microtubule dynamics. J Cell Biol 128:849–862.

Parsons SF, Salmon ED. 1997. Microtubule assembly in clarified *Xenopus* egg extracts. Cell Motil Cytoskeleton 36:1–11.

Pryer N., Walker RA, Skeen VP, Bourns BD, Soboeiro MF, Salmon ED. 1992. Microtubule-associated proteins modulate microtubule dynamic instability in vitro: real-time observations using video microscopy. J Cell Sci 103:965–976.

Sammak PJ, Borisy GG. 1988. Direct observation of microtubule dynamics in living cells. Nature (Lond) 332:724–726.

Saxton WM, Stemple DL, Leslie RJ, Salmon ED, Zavortink M, McIntosh JR. 1984. Tubulin dynamics in cultured mammalian cells. J Cell Biol 99: 2175–2186.

Shiina NT, Moriguchi T, Ohta K, Gotoh Y, Nishida E. 1992. Regulation of a major microtubule-associated protein by MPF and MAP kinase. EMBO J 11:3977–3984.

Stewart-Savage J, Grey RD. 1982. The temporal and spatial relationships between cortical contraction, sperm tail formation, and pronuclear migration in fertilized *Xenopus* eggs. Wilhelm Roux's Arch. Dev Biol 191:241–245.

Tanaka EM, Kirschner MW. 1991. Microtubule behavior in the growth cones of living neurons during axon elongation. J Cell Biol 115:345–363.

Tournebize R Andersen SSL, Verde F, Doree M, Karsenti E, Hyman A. 1997. Distinct roles of PP1 and PP2A-like phosphatases in control of microtubule dynamics during mitosis. EMBO J 16:5537–5549.

Tournebize R, Ashford AJ, Popov A, Karsenti E, Hyman A. 1998. Regulation of microtubule dynamics by XMAP215 in *Xenopus* egg extracts. Mol Biol Cell 9:414a.

Trinczek B, Biernat J, Baumann K, Mandelkow E-M, Mandelkow E. 1995. Domains of tau protein, differential phosphorylation, and dynamic instability of microtubules. Mol Biol Cell 6:1887–1902.

Vandecandelaere A, Pedrotti B, Utton MA, Calvert RA, Bayley PM. 1996. Differences in the regulation of microtubule dynamics by microtubule-associated proteins MAP1B and MAP2. Cell Motil Cytoskeleton 35:134–146.

Vasquez RJ, Gard DL, Cassimeris L. 1994. XMAP from *Xenopus* eggs promote rapid plus end assembly of microtubules and rapid microtubule polymer turnover. J Cell Biol 127:985–993.

Verde F, Dogterom M, Stelzer E, Karsenti E, Leibler S. 1992. Control of microtubule dynamics and length by cyclin A- and cyclin B-dependent kinases in *Xenopus* egg extracts. J Cell Biol 118:1097–1108.

Walczak CE, Mitchison TJ, Desai A. 1996. XKCM1: A *Xenopus* kinesin-related protein that regulates microtubule dynamics during mitotic spindle assembly. Cell 84:37–47.

Walker RA, O'Brien ET, Pryer NK, Soboeiro MF, Voter WA, Erickson HP, Salmon ED. 1988. Dynamic instability of individual, MAP-free microtubules analyzed by video light microscopy: Rate constants and transition frequencies. J Cell Biol 107:1437–1448.

Waterman-Storer C, Gregory J, Parsons SF, Salmon ED. 1995. Membrane/microtubule tip attachment complexes (TACs) allow the assembly dynamics of plus ends to push and pull membranes into tubulovesicular networks in interphase *Xenopus* egg extracts. J Cell Biol 130:1161–1169.

Witman G. 1986. Isolation of *Chlamydomonas* flagella and flagellar axonemes. Methods Enzymol 134:280–290.